

Supplementary Information

NAP1-Related Protein 1 (NRP1) has multiple interaction modes for chaperoning histones H2A-H2B

Qiang Luo^{1,†}, Baihui Wang^{1,†}, Zhen Wu¹, Wen Jiang¹, Yueyue Wang², Kangxi Du¹, Nana Zhou¹, Lina Zheng², Jianhua Gan³, Wen-Hui Shen^{1,4}, Jinbiao Ma^{2,*}, Aiwu Dong^{1,*}

¹State Key Laboratory of Genetic Engineering, Collaborative Innovation Center of Genetics and Development, International Associated Laboratory of CNRS-Fudan-HUNAU on Plant Epigenome Research, Department of Biochemistry, Institute of Plant Biology, School of Life Sciences, Fudan University, Shanghai 200438, PR China

²State Key Laboratory of Genetic Engineering, Collaborative Innovation Center of Genetics and Development, Department of Biochemistry, Institute of Plant Biology, School of Life Sciences, Fudan University, Shanghai 200438, PR China

³Shanghai Public Health Clinical Center, State Key Laboratory of Genetic Engineering, Collaborative Innovation Center of Genetics and Development, Department of Physiology and Biophysics, School of Life Sciences, Fudan University, Shanghai 200438, China

⁴Institut de Biologie Moléculaire des Plantes, UPR2357 CNRS, Université de Strasbourg, 12 rue du Général Zimmer, 67084 Strasbourg Cédex, France

[†]Q.L. and B.W. contributed equally to this work.

*Correspondence: aiwudong@fudan.edu.cn and majb@fudan.edu.cn

This PDF file includes:

Materials and Methods

Supplementary Figures 1-9

Supplementary Tables 1-3

Materials and Methods

Protein expression and purification

The open reading frames (ORFs) encoding Arabidopsis NRP1, H2A (HTA1; AT5G54640) and H2B (HTB1; AT1G07790) have been described previously (1). The ORFs encoding Arabidopsis H3 (AT5G65360), truncated or mutated H2A and H2B, truncated or mutated NRP1 were generated by PCR or overlapping PCR methods (Table S3). The optimized ORFs encoding Arabidopsis H4 (AT2G28740) and DDM1 (AT5G66750) were synthesized by GENEWIZ company (<https://www.genewiz.com.cn/>). The DNA fragments for co-expression of Arabidopsis H3 and H4 were cloned into pETduet-1 vector (Novagen, <http://www.merckmillipore.com>). The DNA fragments encoding full-length, truncated or mutated H2A and H2B were individually cloned into pET28a vector (Novagen, <http://www.merckmillipore.com>). After addition of a DNA fragment encoding a 6×His-SUMO tag, DNA fragments encoding full-length, truncated or mutated NRP1 and DDM1 were individually subcloned into pET28a vector (Table S3).

The recombinant full-length, truncated or mutated NRP1 proteins and DDM1 were expressed in *Escherichia coli* strain BL21 (DE3). The recombinant H3 and H4, and full-length, truncated or mutated H2A and H2B were co-expressed also in BL21 (DE3) (1). In brief, for the purification of full-length, truncated or mutated NRP1 and DDM1, the supernatant was loaded onto a Ni-NTA column. The eluted sample was dialyzed and cleaved by Ulp1 to remove the 6×His-SUMO tag. The proteins were further purified with Superdex 200 16/60 or Superdex 75 16/60 preparation grade columns (GE

Healthcare, USA), then concentrated and stored in a buffer composed of 20 mM Tris-HCl and 150 mM NaCl (pH 8.0). For the purification of full-length, truncated or mutated H2A-H2B proteins, the supernatant was sequentially purified by SP FF cation exchange column and Superdex 75 16/60 preparation grade column. The purified H2A-H2B proteins were stored in a buffer containing 20 mM Tris-HCl and 1 M NaCl (pH 8.0). For the purification of co-expressed H3-H4, the supernatant was purified by SP FF cation exchange column and the contaminated nucleic acids were removed by Butyl column (scanty water column). The co-expressed H3-H4 proteins were further purified by Superdex 200 16/60 preparation grade column, and stored in a buffer containing 20 mM Tris-HCl and 1 M NaCl (pH 8.0).

Crystallization and structure determination

To generate the co-crystal of NRP1-H2A-H2B complex, 15 mg/mL NRP1 (amino acids 19–255) and 24 mg/mL of H2A-H2B heterodimer in 20 mM Tris-HCl (pH 8.0) and 150 mM NaCl were mixed at the molar ratio of 1:2. The crystals were grown in 1 M NaCl, 0.1 M sodium cacodylate, 30% (v/v) PEG 600 and 10% (v/v) glycerol (pH 6.5) at 18 °C. The peptides of NRP1 CTAD, HsNAP1 CTAD-1, HsNAP1 CTAD-2 and their mutants were synthesized by Beijing Scilight Biotechnology LLC (<http://scilight-peptide.com/EN/index.aspx>) (Table S2). To generate NRP1 CTAD-H2A-H2B and HsNAP1 CTAD-H2A-H2B complexes, 15 mg/mL of H2A-H2B in 20 mM Tris-HCl and 150 mM NaCl (pH 8.0) were mixed with 1 mM of the corresponding peptides. The NRP1 CTAD-H2A-H2B crystals were grown in 0.2 M sodium nitrate, 0.1 M Bis-Tris

propane and 20% (w/v) PEG 3350 (pH 8.5). The HsNAP1 CTAD-1-H2A-H2B crystals were grown in 0.7 M ammonium dihydrogen phosphate, 0.07 M sodium citrate and 30% (v/v) glycerol (pH 5.6), while the HsNAP1 CTAD-2-H2A-H2B crystals were grown in 0.2 M sodium acetate and 20% (w/v) PEG 3350 (pH 5.5). Crystals were flash-frozen in the mother solution supplemented with 25% glycerol. Diffraction data were collected at Shanghai Synchrotron Radiation Facility beamlines 17U, 18U and 19U and processed with HKL2000 and HKL3000 packing (<http://www.hkl-xray.com/>). All structures were solved by the molecular replacement method using the Phaser program embedded in the CCP4i suite, with the structures of Arabidopsis NRP1 (PDB:5DAY) (1) and *Xenopus laevis* H2A-H2B (PDB:1AOI) (2) used as search models. Model building and structure refinement were performed with COOT (3) and Phenix (4), respectively. Structural visualization was performed using Pymol (<http://pymol.sourceforge.net/>). The electrostatic potential of NRP1 and H2A-H2B was calculated by Pymol software under the default settings.

Chemical cross-linking and mass spectrometry

NRP1 and H2A-H2B proteins were mixed at the molar ratio of 1:3, incubated at 4 °C for 30 min, and diluted to a final concentration of 0.6 µg/µL with cross-linking buffer containing 20 mM HEPES and 150 mM NaCl (pH 7.5). Cross-linking reactions were performed by adding DSS (disuccinimidyl suberate) or BS3 (bissulfosuccinimidyl suberate) to different concentrations, incubated at 25 °C for 30 min and quenched with 20 mM Tris-HCl (pH 8.0). One third of each cross-linked product was used for SDS-

PAGE analysis, and the remaining was reduced with DTT, alkylated with Iodoacetamide and digested with trypsin. The tryptic peptides were acidified with 1% FA and submitted to LC-MS/MS analysis by an easy nLC 1200 system coupled to Orbitrap Fusion Lomus mass spectrometer (Thermo Fisher Scientific, USA). A one-column system was adopted for all analyses with a 60-min LC gradient. Data-dependent analysis was employed in MS analysis. The most intense ions in 3s were fragmented in HCD mode, and precursors of +1, +2 or unknown charge state were excluded. Raw data were analyzed by pLink 2 software (version 2.3.5) to extract the information of cross-linked peptides.

Isothermal titration calorimetry (ITC)

ITC experiments were performed at 25 °C using a MicroCal iTC200 microcalorimeter. Before the reactions, all proteins and peptides were dialyzed against buffer containing 20 mM HEPES and 150 mM NaCl (pH 7.5). Typically, titrations were carried out using an initial injection volume of 0.5 μL (omitted from the analysis) followed by 30 1.2 μL injections. Data were analyzed using Origin 7 software, and the heat of dilution was subtracted from the raw values. Dissociation constant (K_d) and stoichiometry (N) values were calculated by fitting the isotherm. At least two independent replicates for the ITC experiments have been performed, and the reported error indicates the fit error.

Plant rescue assay

The DNA fragments encoding full-length wild-type or mutated NRP1 were fused to a DNA fragment encoding EYFP, then cloned into the pER8 vector driven by an estradiol-inducible promoter. The resulted constructs of ES::EYFP-NRP1 and ES::EYFP-NRP1 mN (NRP1 mN: NRP1 1-255 E36A/D39A/D40A/K43A, Table S1) were transformed into *nrp1-1 nrp2-1* double mutant plants, respectively. The stable 3rd transgenic Arabidopsis were used for phenotype analysis. Plant growth conditions and Western blotting assay by using GFP antibody (Abmart M20004S) are the same as described previously (1).

Circular Dichroism (CD)

CD analysis was performed with a Chirascan V100 system. All spectra were collected under nitrogen atmosphere at 10-mm path-length, 1-nm bandwidth, 140-nm/min scanning speed and room temperature. Proteins were resolved in PBS buffer, pH7.4. For NRP1 19-77 and its mutant, protein concentration was 0.25 mg/ml, and for NRP1 78-225, NRP1 1-255, NRP1 19-225, histone H2A-H2B and their mutants, protein concentration was 0.1 mg/ml. The spectra were measured two times, averaged and smoothed. The final presented curves were generated by OriginPro 8.

Size-exclusion chromatography with multi-angle light scattering (SEC-MALS)

SEC-MALS was performed at room temperature with a Dawn Heleos MALS detector (Wyatt Technology). The column (Superdex 75 10/300, GE Healthcare) was attached into the system and was pre-equilibrated with buffer containing 20 mM Tris-HCl and

150 mM NaCl (pH8.0). 100 μ L samples (5 mg/ml) were injected on to the column and eluted with the same buffer. The system was normalized by Bovine Serum Albumin (BSA, Sigma-Aldrich).

Electrophoretic mobility shift assay (EMSA) competition assay

A 21-bp DNA duplex was prepared by mixing and annealing two complementary DNA strands (5'-GAAAATGCGGTTGGAGAATTA-3' and 5'-TAATTCTCCAACCGCATTTTC-3') in buffer containing 20 mM Tris-HCl, 150 mM NaCl and 2 mM DTT (pH 7.5). DNA (1 μ M) was mixed with increasing H2A-H2B (1, 2, 3, 4 μ M) in 20 mM Tris-HCl, 150 mM NaCl and 2 mM DTT (pH 7.5). 10 μ L DNA (2 μ M) and H2A-H2B (8 μ M) in 20 mM Tris-HCl, 150 mM NaCl and 2 mM DTT (pH 7.5) were pre-incubated for 30 min, then mixed with increasing wild-type or mutated NRP1 proteins (1, 2, 3, 4, 5, 6, 7, 8 μ M, respectively). The final reaction volume of each sample was 20 μ L. The samples were incubated on ice for 30 min. After reaction, the samples were analyzed by 6% native PAGE gel in 0.5 \times TBE running buffer at 4 $^{\circ}$ C. The gels were stained with GelRed. All reactions were performed at least three times.

EMSA nucleosome assembly assay

The 187-bp DNA containing a core Widom 601 sequence was generated by PCR method. The reconstruction methods of nucleosome and tetrasome were described as previously (5). In brief, 10 μ g octamer and H3-H4 tetramer composed of Arabidopsis recombinant histones were mixed with 10 μ g 187-bp DNA in a buffer containing 10

mM Tris-HCl, 2 M NaCl, 1 mM EDTA and 1 mM DTT (pH 8.0), respectively. The samples were incubated at 4 °C for two hours, then gradually diluted to the salt concentration of 0.6 M by adding TE buffer (10 mM Tris-HCl and 1 mM EDTA, pH 8.0), and kept at 4 °C overnight. Samples were collected after the final dialysis for 4 h in HEN buffer (10 mM HEPES, 1 mM EDTA, 150 mM NaCl, pH7.5). Firstly, wild-type and mutated NRP1 proteins (1 μM) were respectively mixed with increasing amount of H2A-H2B (0.06, 0.12, 0.18, 0.24 μM) in HEN buffer for 30 min at 4 °C; then (H3-H4)₂-DNA tetrasomes were added and incubated on ice for 30 min. After reaction, the samples were analyzed by 6% native PAGE gel in 0.5× TBE running buffer at 4 °C, and the gels were stained with GelRed.

EMSA nucleosome disassembly assay

The 146-bp Widom 601 DNA was synthesized by GENEWIZ company and cloned into pMD19 T-vector. The 229-bp DNA fragment containing a core 146-bp 601 segment at the center was generated by PCR method. The nucleosomes and tetrasomes composed of Arabidopsis recombinant histones and 229-bp DNA were reconstructed as above nucleosome assembly assay. Nucleosome disassembly assay was similar to a previous study (6). The reconstructed nucleosomes were mixed with ATP (1 mM) and DDM1 (10 nM), subsequently incubated with increasing wild-type and mutated NRP1 proteins (4, 8, 12, 16 μM), respectively, and kept at 25 °C overnight. After reaction, the samples were analyzed by 6% native PAGE gel in 0.5× TBE running buffer at 4 °C. The gels were stained with GelRed.

Plasmid supercoiling assay

Arabidopsis recombinant core histones (300 ng H2A-H2B, 300 ng H3-H4) were incubated respectively with wild-type and mutated NRP1 proteins (3 μ g) in buffer containing 10 mM Tris-HCl and 150 mM NaCl (pH 8.0) to a final volume of 25 μ L at 25 $^{\circ}$ C for 30 min. At the same time, relaxed plasmids were obtained from supercoiled p174 RF1 plasmids (500 ng, NEB) treated with topoisomerase I (2 U, Takara) in buffer containing 35 mM Tris, 72 mM KCl, 5 mM MgCl₂, 5 mM DTT, 5 mM spermidine and 0.1 mg/ml BSA (pH 8.0) at 37 $^{\circ}$ C for 30 min. Then relaxed plasmids (20 μ L) were added to the mixture of wild-type or mutated NRP1 proteins and core histones (25 μ L), and incubated at 25 $^{\circ}$ C for 80 min. After that, 50 μ L of stop buffer (20 mM Tris, 20 mM EDTA, 1% SDS and 0.5 mg/ml proteinase K, pH 8.0) was added to stop the above reaction at 25 $^{\circ}$ C for 20 min. Finally, plasmids purified with phenol/chloroform and precipitated with ethanol were analyzed on 1% agarose gel in 1 \times TAE buffer. The gels were visualized by GelRed staining.

Supplementary Figures

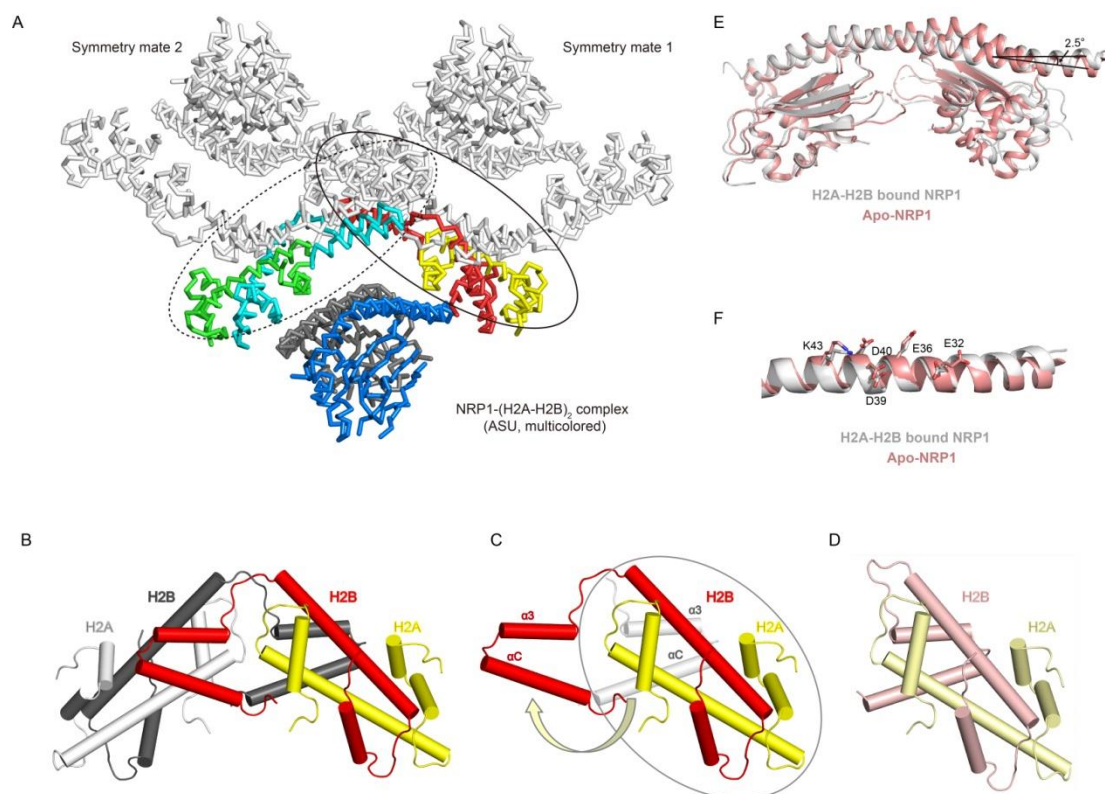


Fig. S1. The conformational comparisons of H2A-H2B or NRP1 in the complex and in the apo structures.

(A) Packing of NRP1-H2A-H2B complexes in the crystal lattice. An asymmetric unit (ASU) of NRP1-(H2A-H2B)₂ is multicolored, and the two symmetry-related complexes (symmetry mate 1 and 2) are colored in white. NRP1-(H2A-H2B)₂ is connected to symmetry mate 1 and 2 by domain swapping between two adjacent H2A-H2B (encircled in ovals).

(B) Two H2A-H2B heterodimers form a H2A-H2B tetramer in (A), in which two H2B are domain-swapped. The H2A-H2B heterodimer in the NRP1 complex structure is shown in yellow and red, and that in symmetry mate 1 or 2 is shown in grey and black.

(C) The H2A-H2B heterodimer in the NRP1 complex structure is shown in yellow and red. The canonical H2A-H2B heterodimer as observed in the apo H2A-H2B is outlined in the oval, in which the domain swapped $\alpha 3$ and αC of H2B are shown as light grey. The curved arrow indicates how domain swap occurs.

(D) The structure of apo H2A-H2B (similar to those in nucleosomes) is the same as the domain-swapped H2A-H2B in (C).

(E) Superposition of NRP1 bound to H2A-H2B with the apo NRP1 structure (PDB: 5DAY). NRP1 dimers in the apo and complex structures are colored in pink and grey, respectively.

(F) Conformational changes of NRP1 key residues involved in H2A-H2B binding in

(E).

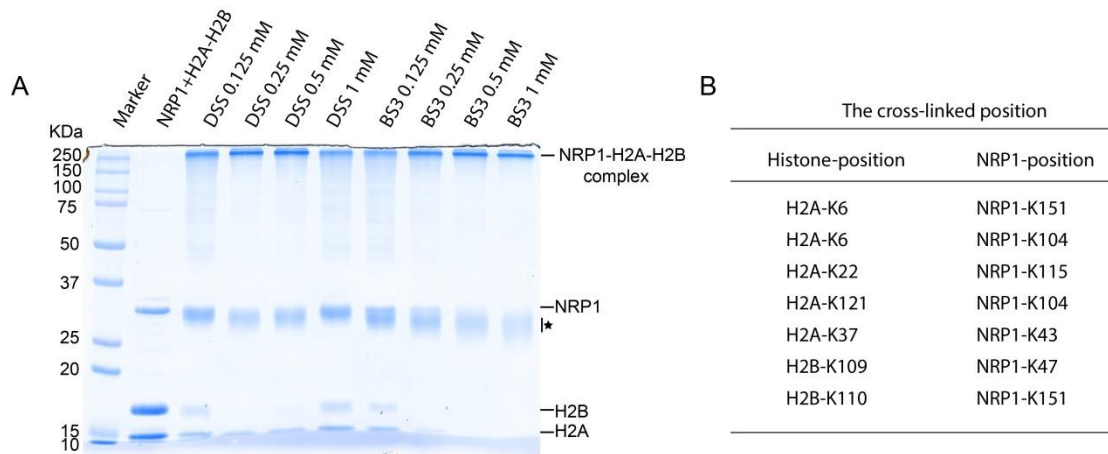


Fig. S2. Cross-linking analysis between NRP1 and H2A-H2B.

(A) SDS-PAGE of cross-linked NRP1 and H2A-H2B. NRP1 dimer was incubated with H2A-H2B at the molar ratio of 1:3 to reach a final concentration $0.6 \mu\text{g}/\mu\text{L}$. The concentrations of DSS and BS3 are indicated in the gel. The cross-linked H2A-H2B dimer was indicated by black star.

(B) A summary of residues cross-linked between NRP1 and histone H2A or H2B. The table only shows the residues cross-linked by both DSS (0.25 mM) and BS3 (0.25 mM) treatments.

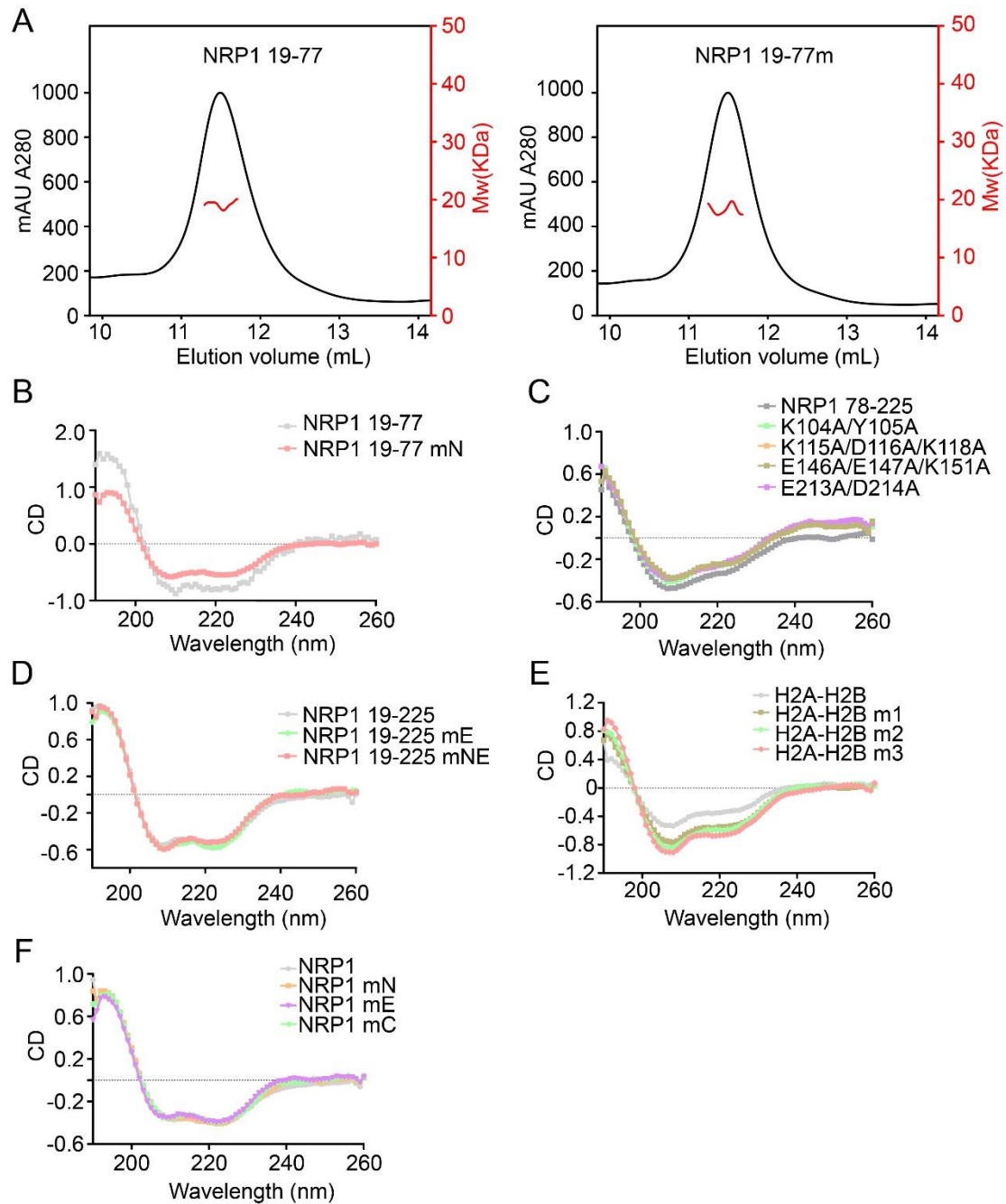


Fig. S3. SEC-MALS and CD spectroscopy analyses for NRP1 and H2A-H2B mutant proteins.

(A) Dimerization of NRP1 19-77 and NRP1 19-77 mN was determined by SEC-MALS.

The molecular weights of NRP1 19-77 and NRP1 19-77 mN were evaluated by the elution profile of analytical SEC-MALS. The measured molecular weights of NRP1

19-77 and NRP1 19-77 mN correspond to a dimer, for the corresponding theoretical weights of NRP1 19-77 and NRP1 19-77 mN dimers are 14.2 KDa and 13.8 KDa, respectively.

(B)-(F) The proper folding in solution of NRP1 and H2A-H2B mutant proteins was determined by CD spectroscopy.

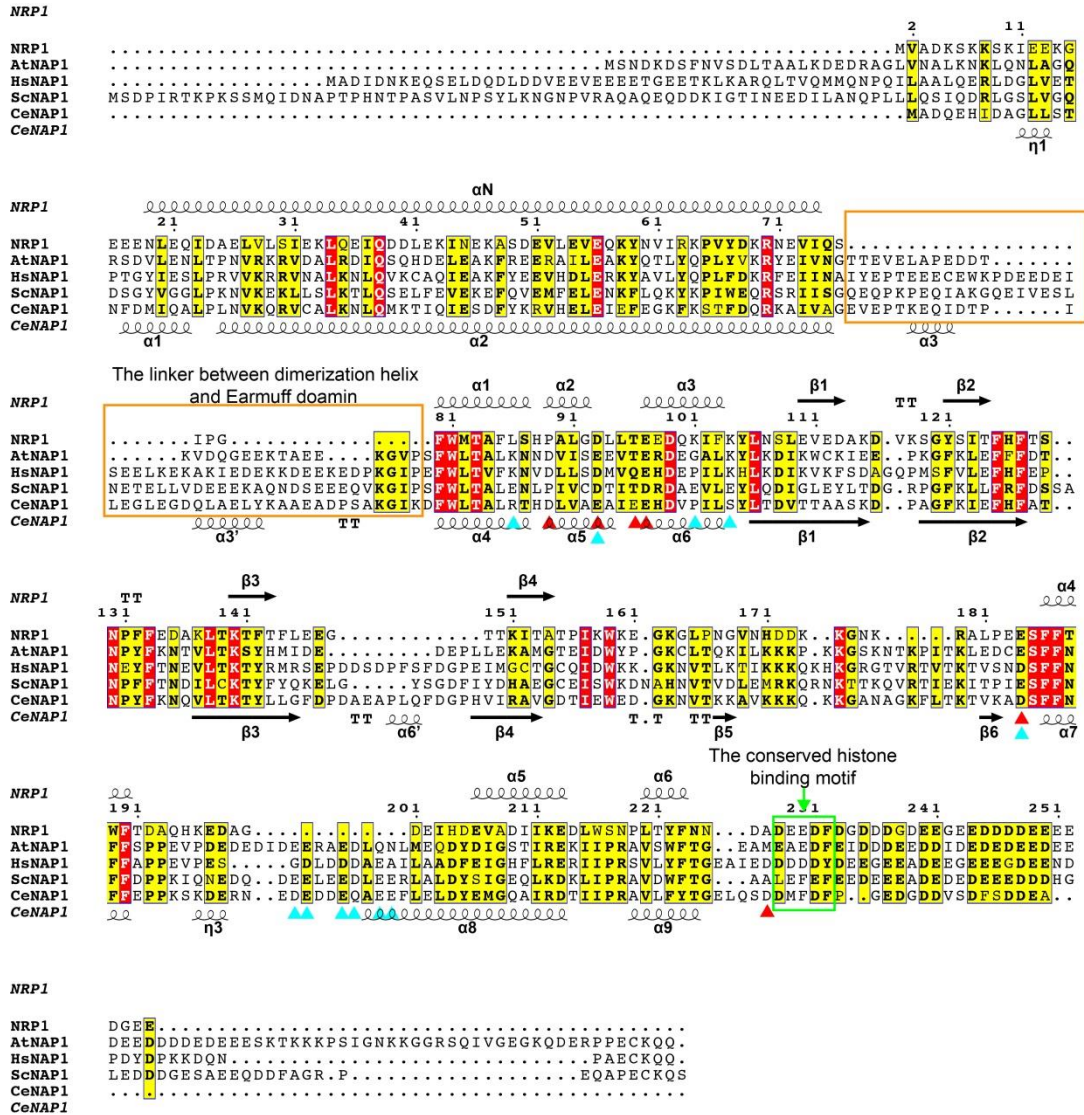


Fig. S4. Sequence alignment of NAP1 proteins from *Arabidopsis thaliana* (At), *Homo sapiens* (Hs), *Saccharomyces cerevisiae* (Sc) and *Caenorhabditis elegans* (Ce). The identical and similar residues are shown in red and yellow fonts, respectively. The residues important for H2A-H2B binding within CeNAP1 and ScNAP1 are indicated by red and cyan angles, respectively. The linker region between NRP1 α N and earmuff domains of NRP1 is outlined with a brown box and the conserved histone binding motif at the C-terminal region is highlighted with a green box.

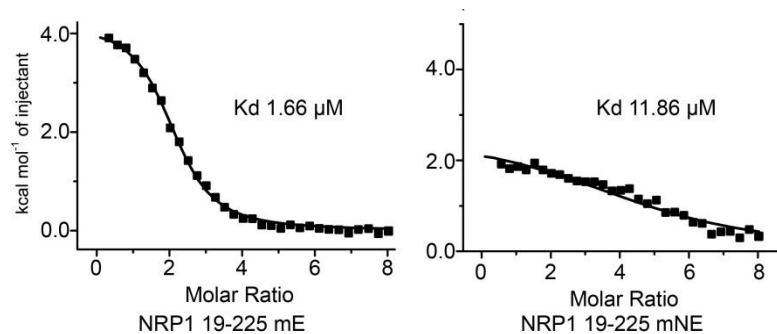


Fig. S5. The binding affinities between H2A-H2B and NRP1 19-225 mE (NRP1 19-225 K115A/D116A/K118A/E213A/D142A) or NRP1 19-225 mNE (NRP1 19-225 E36A/D39A/D40A/K43A/K115A/D116A/K118A/E213A/D142A) are measured by ITC experiment. The NRP1 mutant proteins (600 μ M) are titrated into H2A-H2B (20 μ M).

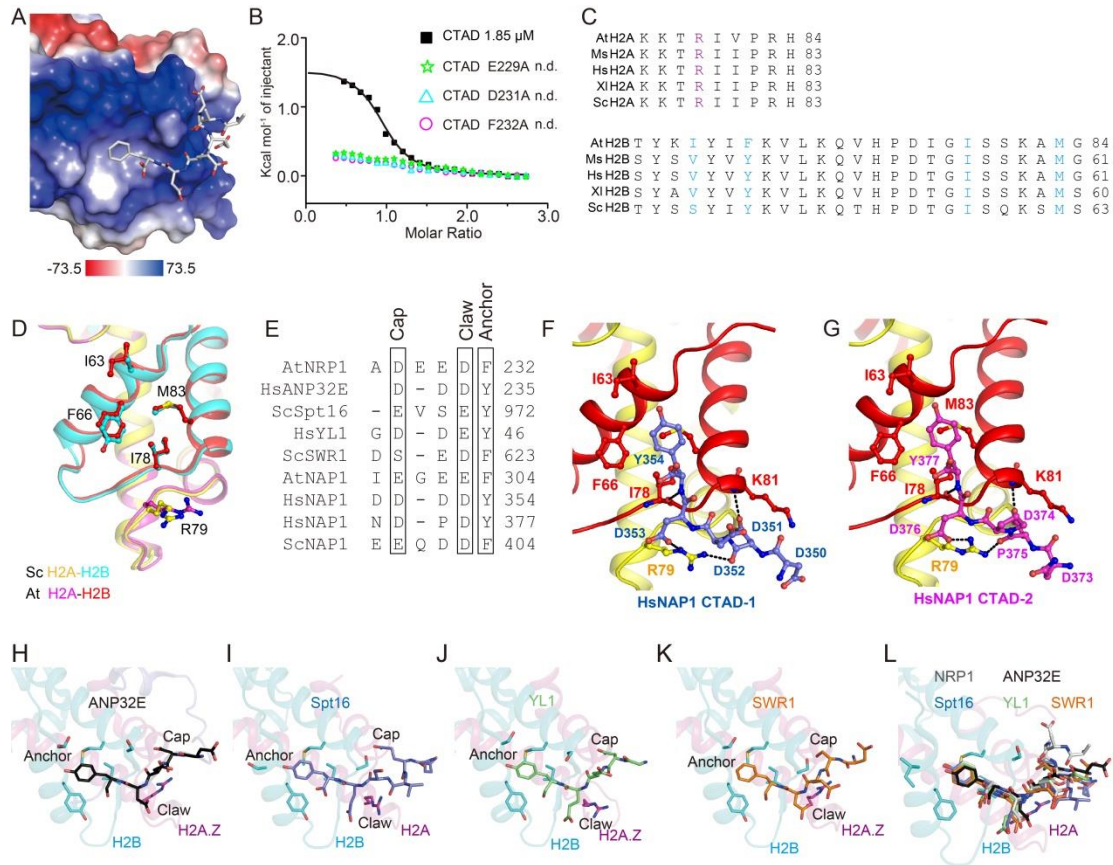


Fig. S6. CTAD domain is a conserved histone binding motif of NAP1 family proteins.

(A) Surface presentation showing the NRP1-CTAD binding pocket within H2A-H2B.

The scale of the electrostatic potential is -73.5 (red) to +73.5 KT/e (blue).

(B) ITC analysis showing the impact of NRP1 CTAD mutations on H2A-H2B binding.

Wild-type and mutated NRP1 CTAD peptides (300 μ M) are titrated into H2A-H2B (20 μ M).

(C) Sequence alignment of H2A and H2B from *Arabidopsis thaliana* (At), *Mus musculus* (Ms), *Homo sapiens* (Hs), *Xenopus laevis* (Xl) and *Saccharomyces cerevisiae* (Sc). The key residues participating in NRP1 CTAD binding are indicated in purple (H2A) and cyan (H2B), respectively.

(D) Structural superposition of the CTAD binding pockets within yeast H2A-H2B (4WNN) and Arabidopsis H2A-H2B (this study). At: *Arabidopsis thaliana*, Sc: *Saccharomyces cerevisiae*.

(E) Sequence alignment of the Cap-Claw-Anchor motifs in NRP1, ANP32E, Spt16, YL1, SWR1 and NAP1 proteins. Hs: *Homo sapiens*, Sc: *Saccharomyces cerevisiae*, At: *Arabidopsis thaliana*.

(F–G) Detailed interactions between H2A-H2B and HsNAP1 CTAD-1 (F) or HsNAP1 CTAD-2 (G).

(H–L) The conserved Cap-Claw-Anchor motifs observed in crystal structures of histone chaperones ANP32E (PDB_ID:4CAY, black) (H), Spt16 (PDB_ID:4WNN, blue) (I), YL1 (PDB_ID:5FUG, green) (J) and chromatin remodeling factor SWR1 (PDB_ID:4M6B, orange) (K) in complexes with H2A-H2B, in which only the conserved E(D)-X/XX-D(E)-F(Y) motifs are shown. The structural superposition of NRP1, ANP32E, Spt16, YL1 and SWR1 (L).

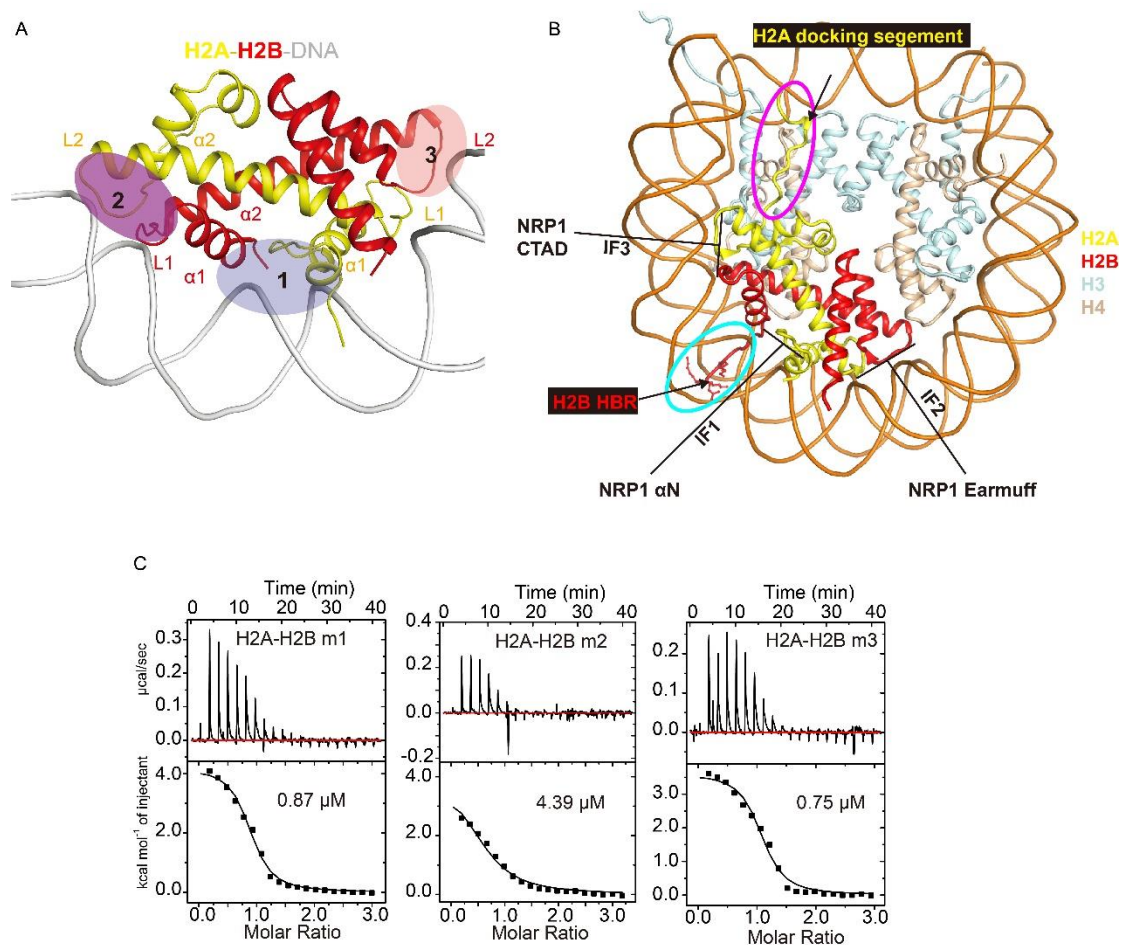


Fig. S7. DNA/NRP1 interacting interfaces of H2A-H2B.

(A) DNA interacting interfaces 1 (IF1), 2 (IF2) and 3 (IF3) of H2A-H2B within a nucleosome.

(B) Diagram showing the overlapping between nucleosomal DNA and α N, earmuff and CTAD domains of NRP1 at DNA interacting interfaces 1, 2 and 3 of H2A-H2B, respectively. The H2A docking segment and the H2B HRB are indicated by magenta and cyan circles, respectively.

(C) ITC experiments showing the impact of H2A-H2B mutations on NRP1 earmuff domain binding. In H2A-H2B m1 (H2A R31A/R34A, H2B E59A/T60A/K62A/I63A/Y64A), H2A α 1 and H2B α 1 within IF1 are mutated. In H2A-H2B m2 (H2A E43A/R44A, H2B K109A/K110A/T112A), H2A L1 and H2B L2 within

IF2 are mutated. In H2A-H2B m3 (H2A K76A/K77A/T78A/R79A), H2A loop 2 (L2) within IF3 is mutated. Titrations were carried out using an initial injection volume of 0.5 μ L (omitted from the analysis) followed by 20 (each 2 μ L) injections.

domain; mC: NRP1 mC (NRP1 1-255 E229A/D231A/F232A), mutation within CTAD domain (Table S1).

(B) NRP1 displays nucleosome disassembly activity in the presence of the chromatin remodeling factor DDM1. The nucleosomes were mixed with increasing NRP1 (0, 4, 8, 12, 16 μ M, lanes 1-5), with chromatin remodeling factor DDM1 (lane 6), with both DDM1 and ATP (lane 7), with DDM1, ATP and increasing NRP1 (lanes 8-11), NRP1 mN (lanes 12-15), NRP1 mE (lanes 16-19) and NRP1 mC (lanes 20-23), respectively. The nucleosomes were indicated by the white arrow, and the DNA-H2A-H2B bands were marked by the red box.

(C) NRP1 promotes H2A-H2B removal from nucleosomes in the presence of DDM1. The reconstructed nucleosomes (lane 1), H3-H4 mixed with DNA (lane 2), nucleosomes mixed with DDM1, ATP and NRP1 (lane 3), H2A-H2B mixed with DNA (lane 4), and the band of DNA-H2A-H2B are marked by the red box.

(D) Compositional analysis of DNA-H2A-H2B in (B). The DNA-H2A-H2B band (lane 11 in B) and the bands (lanes 15,19 and 23 in B) at the corresponding positions were cut and dissolved in 10 mM HEPES, 100 mM DTT and 150 mM NaCl (pH 8.0). H3-H4 (lane 1), H2A-H2B (lane 2), and DNA-H2A-H2B from reactions with NRP1, NRP1 mN, NRP1 mE and NRP1 mC (lanes 3-6) were analyzed by Western blotting assay with antibodies @H2A (Abmart, T55481S) and @H4 (Millipore, 07-108), respectively.

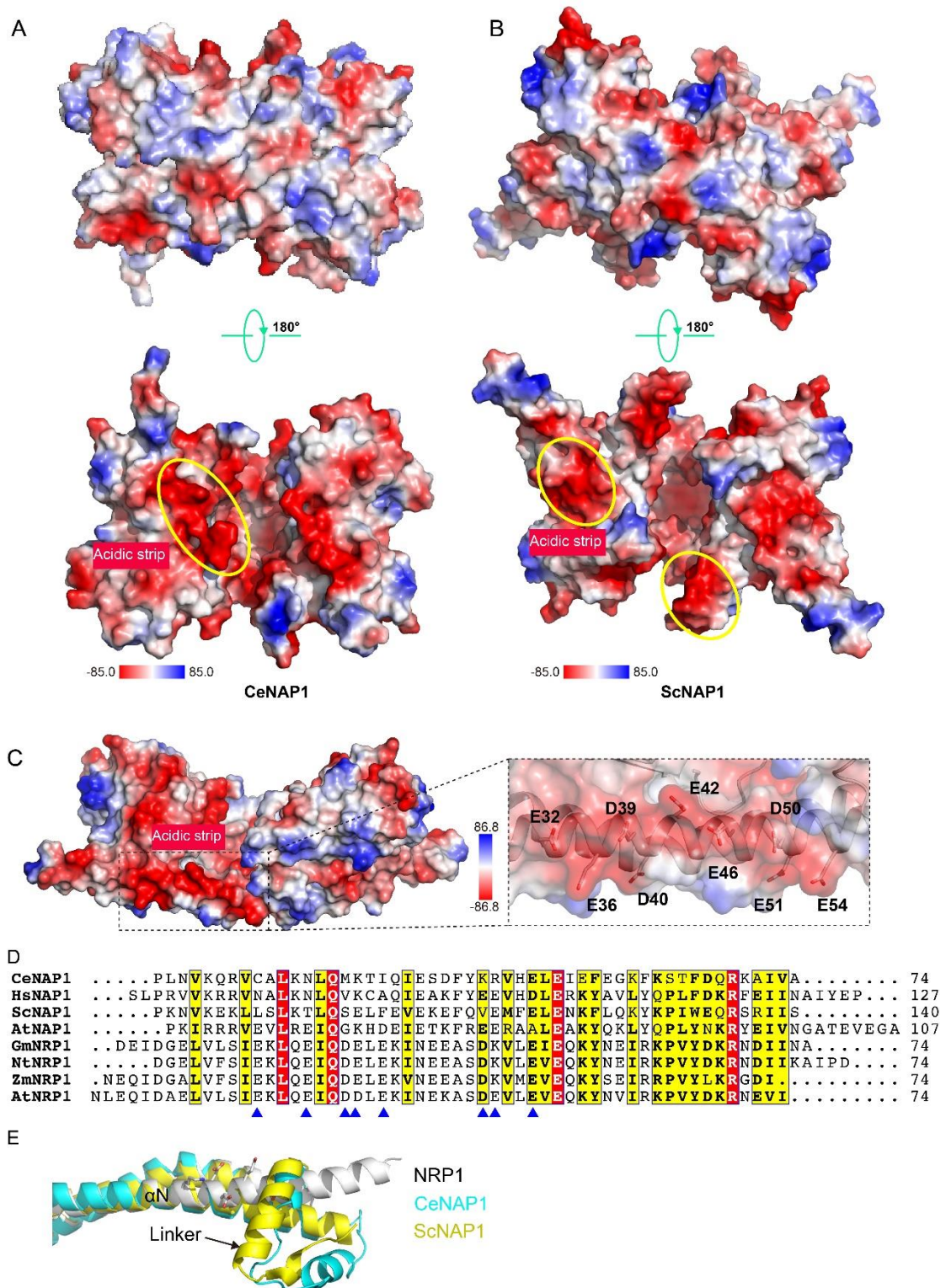


Fig. S9. Acidic strips are important for NAP1 proteins to associate with histones.

(A-B) The electrostatic potential distribution of CeNAP1 (PDB: 6K09) (A) and ScNAP1 (5G2E) (B) in different views. The acidic strips in the concave surfaces are

indicated by yellow circle. Ce: *Caenorhabditis elegans*, Sc: *Saccharomyces cerevisiae*.

The scales of the electrostatic potential are -85 (red) to +85 KT/e (blue) in (A) and -86.8 (red) to +86.8 KT/e (blue) in (B), respectively.

(C) The electrostatic potential distribution of NRP1. The acidic strip of NRP1 α N is highlighted by black box and the detailed acidic residues are labeled in the right panel.

(D) Sequence alignment of α N domains within NAP1 family proteins. The essential residues forming the acidic strip in NRP1 α N are indicated by blue triangles. Hs: *Homo sapiens*, Sc: *Saccharomyces cerevisiae*, At: *Arabidopsis thaliana*, Nt: *Nicotiana tabacum*, Gm: *Glycine max*, Zm: *Zea mays*. Ms: *Mus musculus*, Xl: *Xenopus laevis*.

(E) Structural superposition of NRP1, CeNAP1, and ScNAP1, showing that the histone binding region of NRP1 α N is buried by the longer linkers in CeNAP1 and ScNAP1.

Supplementary Tables

Table S1. Mutants of NRP1 and H2A-H2B

NRP1 mN	E36A/D39A/D40A/K43A
NRP1 mE	K115A/D116A/K118A/E213A/D214A
NRP1 mNE	E36A/D39A/D40A/K43A/K115A/D116A/K118A/E213A/D214A
NRP1 mC	E229A/D231A/F232A
H2A-H2B m1 (DNA interface 1)	H2A R31A/R34A H2B E59A/T60A/K62A/I63A/Y64A
H2A-H2B m2 (DNA interface 2)	H2A E43A/R44A H2B K109A/K110A/T112A
H2A-H2B m3 (DNA interface 3)	H2A K76A/K77A/T78A/R79A

Table S2. Peptides used in this study

Peptides	FW(Da)	Sequence	Catalogue	Application
NRP1 CTAD	839.77	DADEEDF	C07106202	ITC, crystallization
HsNAP1 CTAD-1	885.76	EDDDDDY	C07106401	ITC, crystallization
HsNAP1 CTAD-2	880.83	EENDPDY	C07106501	ITC, crystallization
NRP1 CTAD E229A	781.74	DADAEDF	C07108101	ITC
NRP1 CTAD D231A	795.76	DADEEAF	C07108001	ITC
NRP1 CTAD F232A	763.68	DADEEDA	C07107901	ITC

Table S3. Primers used in this study

Name	Sequence (5'-3')
Primers for NRP1 and H2A-H2B	
NRP1-BamHI-F	ACCAGGATCCGTTGCGGACAAGAGCAAGAAGTCG
NRP1-Sall-R	TACCGTCGACTCATTCTCACCATCTTCTCCTCTTC
NRP1 19-BamHI-F	ACCAGGATCCTTGGAGCAAATCGACGCAGAGCTTGTCT
NRP1 77-Sall-R	TACCGTCGACTCAAATCGATTGGATAACTTCATTGCGCTTGT
NRP1 78-BamHI-F	ACCAGGATCCCCTGGCAAAGGATGACTGCAAAAAGAGTCATC
NRP1 225-Sall-R	TACCGTCGACATTGTTGAAGTAGGTGAGAGGGTTGGACCAGAGATCT
YFP-Sall-F	TACCGTCGACATGGTGAGCAAGGGCGAGGAGCTGTTAC
YFP-NRP1-F	ACTCTCGGCATGGACGAGCTGTACAAGGTTGCGGACAAGAGCAAGAAGT CGAAAA
YFP-NRP1-R	TTTTCGACTTCTTGCTCTGTCCGCAACCTTGTACAGCTCGTCCATGCCGA GAGT
NRP1-SpeI-R	GGACTAGTTCATTCTCACCATCTTCTCCTCTTCATCGT

H2A-NcoI-F2	TAAGAAGGAGATATACCATGGCTGGCTCGTGGA AAAA ACTCTTGATCC
H2A-EcoRI-R	CCGGAATTCGGATCTCTAATCTTCCTGAGGCTTTGAAGCAC
H2B-EcoR-F	CCGGAATTC AATAATTTTGT TTA ACTTTAAGAAGGAGATATACCATGGCAC
H2B-Sall-R2	TGCGGCCCGCAAGCTTGTCTGACTCAAGAGCTAGTAAACTTGGTAACCGCCT TG
H2A 14-106-NcoI-F	CATGCCATGGCAAAGCTACATCTCGGAGTAGCAAAGCCG
H2B 51-148-BamHI-R	CGCGGATCCTCAAGAGCTAGTAAACTTGGTAACCGCCTTGTA
Primers for NRP1 mutants	
NRP1D39A/E36A-F	TTCTCTCAATTGAGAAGCTTCAGGCGATTCAAGCCGACCTCGAGAAGATT AACGAAAAG
NRP1D39A/E36A-R	CTTTTCGTTAATCTTCTCGAGGTCGGCTTGAATCGCCTGAAGCTTCTCAAT TGAGAGAA
NRP1 mN-F	GAAGCTTCAGGCGATTCAAGCCGCCCTCGAGGCGATTAACGAAAAGGCC AGTGAC
NRP1 mN-R	GTC ACTGGCCTTTTCGTTAATCGCCTCGAGGGCGGCTTGAATCGCCTGAA GCTTC
NRP1 K115/D116/K118A-F	CTCTCTGGAAGTGGAGGATGCCGCAGCTGTGGCATCTGGATACTCTATAA CTTTTCA
NRP1 K115/D116/K118A-R	TGAAAAGTTATAGAGTATCCAGATGCCACAGCTGCGGCATCCTCCACTTCC AGAGAG
NRP1 mE-F	TGATGAGGTTGCTGATATTATCAAGGCGGCGCTCTGGTCCAACCTCTCAC C
NRP1 mE-R	GGTGAGAGGGTTGGACCAGAGCGCCGCTTGATAATATCAGCAACCTCAT CA
NRP1 mC-F	ACTTCAACAATGATGCTGATAAAGAGAAGGCTGATGGAGATGATGATGGT GACGAAGAG
NRP1 mC-R	CTCTTCGTCACCATCATCATCTCCATCAGCCTTCTCTTTATCAGCATCATTGT TGAAGT
NRP1K104A/Y105A-F	CCTCTTGACTGAAGAAGACCAAAGATTTTTCGCGCCTTGA ACTCTCTGG AAGTGGAG
NRP1K104A/Y105A-R	CTCCACTTCCAGAGAGTTCAAGGCCGCAAAAATCTTTTGGTCTTCTTCAG TCAAGAGG
NRP1K115A/D116A/K1 18A-F	CTCTCTGGAAGTGGAGGATGCCGCAGCTGTGGCATCTGGATACTCTATAA CTTTTCA
NRP1K115A/D116A/K1 18A-R	TGAAAAGTTATAGAGTATCCAGATGCCACAGCTGCGGCATCCTCCACTTCC AGAGAG
NRP1E146A/E147A/K15 1A-F	ACCAAGACATTTACTTTCCTTG CAGCAGGAACAACAGCAATCACTGCAAC TCCTATCAA
NRP1E146A/E147A/K15 1A-R	TTGATAGGAGTTGCAGTGATTGCTGTTGTTCTGCTGCAAGGAAAGTAAA TGCTTTGGT
NRP1D213A/E214A-F	GATGAGGTTGCTGATATTATCAAGGCAGCTCTCTGGTCCAACCTCTCACC T
NRP1D213A/E214A-R	AGGTGAGAGGGTTGGACCAGAGAGCTGCCTTGATAATATCAGCAACCTC

	ATC
Primers for H2A-H2B mutants	
H2AR31A/R34A-F	CGGTCTTCAATTCCCGGTGGGTGCTATCGCTGCTTTCTTAAAAGCCGGTAA ATACGCC
H2AR31A/R34A-R	GGCGTATTTACCGGCTTTTAAGAAAGCAGCGATAGCACCCACCGGAATT GAAGACCG
H2AE43A/R44A-F	CTTAAAAGCCGGTAAATACGCCGAGCTGTTGGTGCCGGTGCTCCGGTTT
H2AE43A/R44A-R	AAACCGGAGCACCGGCACCAACAGCTGCGGCGTATTTACCGGCTTTTAA G
H2AK76A/K77A/T78A/R 79A-F	GAAACGCAGCAAGAGACAACGCGGCGGCAGCTATTGTTCTCGTCACAT TCAG
H2AK76A/K77A/T78A/R 79A-R	CTGAATGTGACGAGGAACAATAGCTGCCGCCGCGTTGTCTCTTGCTGCGT TTC
H2BE59/T60/K62/I63/Y 64A-F	CGATCTAAGAAAAACGTCGCAGCCTACGCGCCTTCATCTCAAGGTGCT GAAGCAGGT
H2BE59/T60/K62/I63/Y 64A-R	ACCTGCTTCAGCACCTGAAGATGAAGGCCGCGTAGGCTGCGACGTTTTT CTTAGATCG
H2BK109A/K110A/T112 A-F	TTCGAACTCGCTAGGTACAACGCGGCCGCGCCATTACATCTCGCGAGA TCCAG
H2BK109A/K110A/T112 A-R	CTGGATCTCGGAGATGTAATGGCCGCGCCGCGTTGTACCTAGCGAGTT TCGAA
Primers for tetrasome/nucleosome reconstruction	
187bp-F	CTCGGGTGATGCCGGATCCCCT
187bp-R	CAAGCGACACCGGCACTGGAAC
229bp-F	CATGATTACGCCAAGTTTGCACGCCTGCCG
229bp-R	CCAGTGAATTAGAACTCGGTACGCGCGGAT

References

1. Zhu Y, *et al.* (2017) The Histone Chaperone NRP1 Interacts with WEREWOLF to Activate GLABRA2 in Arabidopsis Root Hair Development. *Plant Cell* 29(2):260-276.
2. Luger K, Mader AW, Richmond RK, Sargent DF, & Richmond TJ (1997) Crystal structure of the nucleosome core particle at 2.8 Å resolution. *Nature* 389(6648):251-260.
3. Emsley P, Lohkamp B, Scott WG, & Cowtan K (2010) Features and development of Coot. *Acta crystallographica. Section D, Biological crystallography* 66(Pt 4):486-501.
4. Adams PD, *et al.* (2010) PHENIX: a comprehensive Python-based system for macromolecular structure solution. *Acta crystallographica. Section D, Biological crystallography* 66(Pt 2):213-221.
5. Hamiche A & Richard-Foy H (1999) Characterization of specific nucleosomal states by use of selective substitution reagents in model octamer and tetramer structures. *Methods* 19(3):457-464.
6. Lorch Y, Maier-Davis B, & Kornberg RD (2006) Chromatin remodeling by nucleosome disassembly in vitro. *Proceedings of the National Academy of Sciences of the United States of America* 103(9):3090-3093.